Refereed Proceedings

The 12th International Conference on Fluidization - New Horizons in Fluidization Engineering

Engineering Conferences International *Year* 2007

Improved Li-Ion Battery Performance by Coating Cathode Nano-Particles using Atomic Layer Deposition

Renske Beetstra* John Nijenhuis†
Erik M. Kelder‡ J. Ruud van Ommen**

*Delft University of Technology, r.beetstra@tudelft.nl
†Delft University of Technology, j.nijenhuis@tudelft.nl
‡Delft University of Technology, e.m.kelder@tudelft.nl
**Delft University of Technology, j.r.vanommen@tudelft.nl

IMPROVED Li-ION BATTERY PERFORMANCE BY COATING CATHODE NANO-PARTICLES USING ATOMIC LAYER DEPOSITION

Renske Beetstra, John Nijenhuis, Erik M. Kelder and J. Ruud van Ommen
Delft University of Technology - DelftChemTech
Julianalaan 136, 2628 BL Delft, The Netherlands
r.beetstra@tudelft.nl

ABSTRACT

The use of nanoparticles as a cathode in Li-ion batteries is very promising. However, many of the cathode materials that could be economically attractive suffer from degradation. Therefore, an objective is to stabilise the surface, in order to reduce the degradation. A setup was built to coat the nanoparticles by atomic layer deposition in a fluidised bed reactor. The first fluidisation results for the nanoparticles are presented in this paper.

INTRODUCTION

Li-ion batteries have many advantages over other rechargeable batteries. First of all, they have a higher output voltage, 3.6 V, compared to 1.2 V for nickel-cadmium and nickel-metal-hydride batteries. Secondly, the energy density is higher, resulting in smaller and lighter batteries. Other advantages are a low self-discharge, good cycle-life and very low maintenance. Drawbacks are the relatively high costs and long charging times, and the fact that the batteries age in time, whether they are being used or not.

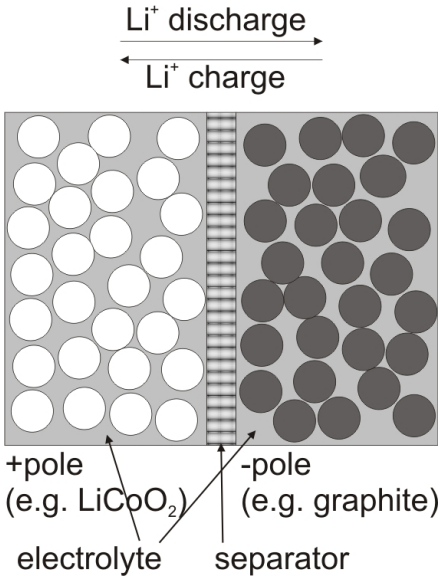

Figure 1: simplified model of a rechargeable Li-ion battery

Published by ECI Digital Archives, 2007

Figure 1 shows a schematic of a rechargeable Li-ion battery. Most commercial Li-ion batteries utilize $LiCoO_2$ or $LiNiO_2$ as cathode materials, and a carbonaceous material as anode. Lithium-ions can occupy positions in both of these materials, but have a different energy in either of the two materials. Anode and cathode materials are separated by an electrolyte, which serves to conduct the Li-ions and is usually a solution of a lithium salt such as $LiPF_6$ in organic solvents, e.g. a mixture of dimethyl carbonate and ethylene

The 12th International Conference on Fluidization - New Horizons in Fluidization Engineering, Art. 44 [2007]

carbonate. During discharge, lithium ions move from anode to cathode, thereby releasing their energy. During charging, the opposite reaction occurs (1).

Recent research activities have been aimed towards the development of new anode materials, whereby especially the spinel-type $Li_4Ti_5O_{12}$ seems to be promising (2, 3). This material has the major advantage that it has a three-dimensional structure for lithium intercalation (the insertion of lithium into the crystal lattice), whereas the layered structure of graphite can only allow lithium transport in two dimensions. High charge and discharge rates are possible with this material. Moreover, it is more electrochemically stable than graphite and therefore safer batteries can be made. The drawback is that the potential at which lithium intercalation occurs is much higher than that for a graphite electrode, about 1.5 V with respect to Li/Li^+, whereas that for graphite is close to the potential of lithium. This results in batteries with a lower output voltage than those using graphite anodes. To overcome this problem, new cathode materials have been developed with higher potentials than the currently used materials. A possible new cathode material is $LiMg_xNi_{0.5-x}Mn_{1.5}O_4$, which is also a spinel. This is cheaper than cobalt materials and has a cathode voltage of 4.7-4.9 V against Li/Li^+. Therefore, the battery output voltage for a $Li_4Ti_5O_{12}/LiMg_xNi_{0.5-x}Mn_{1.5}O_4$ combination could be 3.2-3.4 V, which is an acceptable value (2, 3).

A problem with this cathode material is the dissolution of transition metal ions, especially Mn^{3+}-ions, in the electrolyte (1). When this occurs, the structure of the material changes and there is a smaller number of positions available for lithium intercalation. In addition, the high oxidation ability of Mn^{4+}-ions that are formed during discharge may lead to a decomposition of the solvents in the electrolyte. These factors lead to a capacity loss that is independent of the cycling but proceeds progressively in time. The capacity fading increases with temperature: when Li-ion batteries are stored at temperatures of 60°C, a battery may lose up to 40% of its capacity in only three months time. The problem is more severe for high-voltage materials than for 'regular' cathode materials.

Besides the development of new materials, there is also research dedicated to the use of nanopowders in batteries (3, 4). These powders have several advantages over the current cathode or anode materials. Firstly, the surface area per weight increases strongly, leading to enhanced charge transfer (faster charging). Secondly, the diffusion lengths for Li-ions are very short, which enhances the power performance by increasing the effective capacity for lithium storage. Thirdly, the nanopowders are much more resistant to stresses due to expansion and shrinking during intercalation and deintercalation of the lithium ions, which cause crystal fatigue and loss of capacity in regular cathode materials. The most important drawback of nano-materials in batteries is the increased dissolution of the transition metal ions. This dissolution in the electrolyte is a surface related problem, and therefore increases very fast with decreasing particle size.

Objective

In this research project, we aim to provide the cathode nanoparticles with a coating that prevents the dissolution of transition metal ions in the electrolyte, but does not influence the electrochemical properties of these particles. Thus, the layer should be as thin as possible to let Li-ions diffuse through it, while it should be free of defects to keep the Mn^{3+}-ions in the cathode material. Al_2O_3-coatings have been shown to give

very good results in reduction of the capacity loss for $LiMn_2O_4$-cathodes (5). Other possible materials for the coating are ZnO or other oxides. The layer will be formed by atomic layer deposition in a fluidised bed reactor, as proposd by Wank et al. (6, 7). A second objective is to find optimal conditions for the layer (such as thickness and material) and the process of its formation. In this paper, we will describe the behaviour of the nanopowder during fluidisation.

ATOMIC LAYER DEPOSITION

Atomic Layer Deposition (ALD) is a technique that was developed in the 1970's to form thin layers on solid substrates (8). It was developed originally to produce thin films for electroluminescent displays, but was later adopted for other substrates as well. Ferguson et al. (9) were the first to use this technique on particle substrates. Each ALD-cycle comprises two steps: in the first step a gaseous (usually organometallic) precursor is adsorbed to the surface, which in the second step reacts with a second gas to form a monolayer. The number of cycles determines the thickness of the coating, which as a result is controllable to the atomic level. The quality of the layer is determined by the surface coverage in the adsorption step. When an alumina coating is desired, the precursor could be tri-methyl-aluminium, which reacts with water in the second step.

Performing ALD in a fluidised bed reactor has the advantage that the gas-solid contacting is excellent, and that the particle surfaces are not covered by other particles. Therefore, the precursor will adsorb everywhere on the surface and the deposited layer will be uniform. This was shown by Wank et al. (6, 7). According to the Geldart (10) classification, nanoparticles belong to the C-category and thus, they are very difficult to fluidise due to the large interparticle forces. However, recent research has shown that with addition of energy dynamic clusters can be formed with sizes in the order of 100 μm, which fluidise like A-powders. Energy can be supplied in the form of e.g. (mechanical) vibration (11) or sound (12). Hakim et al. (13)

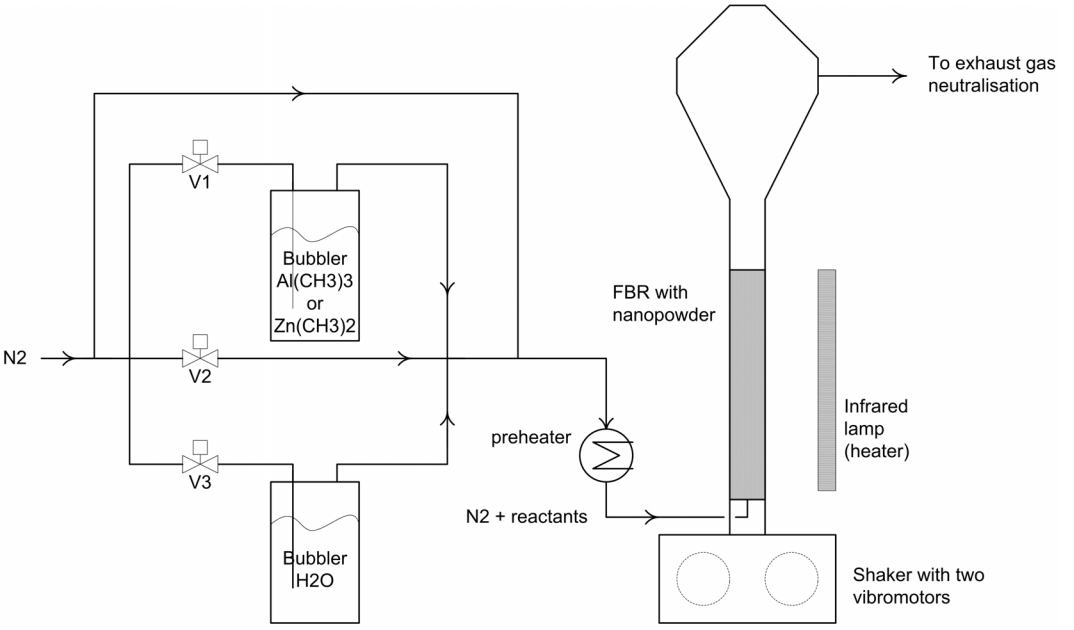

Figure 2: Schematic drawing of the setup for atomic layer deposition in a fluidised bed reactor.

showed that the fluidisation behaviour depends on the properties of the aggregates rather than those of the individual particles and investigated the influence of several variables on these aggregates. They also showed that there are dynamic (soft) aggregates that grow and break up continuously, and static (hard) aggregates that do not change shape or size. The process for particle ALD was patented in three US patents by George et al (14-16).

ALD is different from Chemical Vapour Deposition (CVD) in that the different reactant gases are fed to the sample consecutively instead of at the same time. Therefore, the coatings deposited with ALD are much more uniform than those formed with CVD. Since we are interested in very uniform layers to keep the influence on the electrochemical properties as low as possible, the CVD-process is not suited in this case.

EXPERIMENTAL

Figure 2 shows a schematic drawing of the experimental setup for the ALD-process. It consists of a 26 mm internal diameter, 500 mm long glass reactor tube that is filled with (nano)particles. The reactor is placed on a shaker driven by two vibromotors that produce a low amplitude vibration at adjustable frequency to assist fluidisation. The fluidizing gas is nitrogen. Each ALD-cycle consists of four process steps:

1. Valve V1 is opened, so that part of the nitrogen is led through a bubbler containing the organometallic precursor and saturated with its vapour. This vapour adsorbs on the particle surface.
2. When the complete particle surface is covered with the precursor, V1 is closed and V2 is opened to flush the tubes with pure nitrogen. This prevents (undesired) reactions in the tubes.
3. V2 is closed and V3 opened to lead the gas through a bubbler containing water. The water vapour reacts with the organometal on the surface of the powder.
4. V2 is opened again and V3 closed to clear the tubes for the next cycle.

These steps are repeated until a sufficient number of cycles has been performed to achieve the desired thickness of the coating.

The variables that need to be optimised in the ALD-process are the number of cycles, coating material, overall flow, reactant concentration, cycle times for precursor and water, vibration frequency, reaction temperature etc. During the process the temperature, pressure difference and pressure fluctuations are recorded.

For the experiments described in this paper, only the fluidisation part of the set-up has been used, i.e. gas without reactants for the fluidisation, assisted by vibration. Two types of particles were used: the first type is the $LiMg_{0.05}Ni_{0.45}Mn_{1.5}O_4$ cathode material, which was prepared by the auto-ignition method as described by Lafont et al. (3). Figure 3 shows TEM (transmission electron microscope) pictures of this material. The particle dimensions observed in these TEM-images are 20-100 nm. A BET-analysis rendered a surface of 6.4 m^2/g, from which an equivalent diameter of 213 nm can be calculated. Laser diffraction showed a very wide particle size distribution, ranging from 40 nm or smaller (40 nm is the lower limit of the apparatus) to 60 µm (clusters). Combination of these measurements leads to the conclusion that the particles form clusters, and that part of the clusters are ‘hard’ aggregates, with necking between the primary particles. To make a comparison possible, also a more

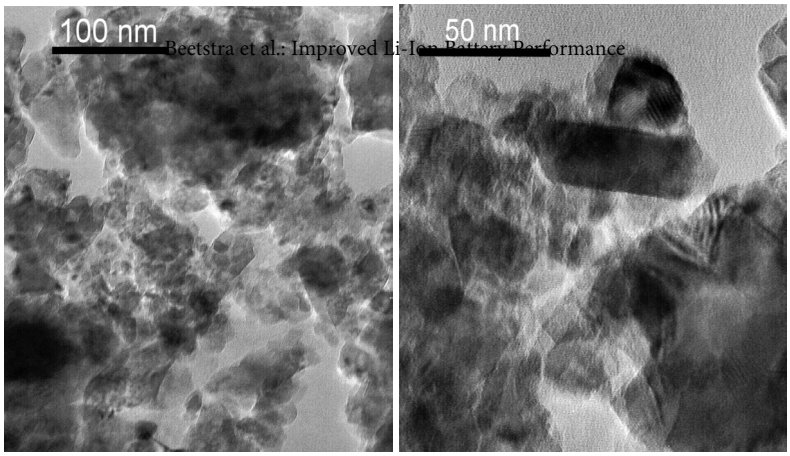

Figure 3: TEM-picture of nanocrystalline $LiMg_{0.05}Ni_{0.45}Mn_{1.5}O_4$ cathode material

common type of nanoparticles has been investigated: commercial titania particles. These particles have a diameter of 20-25 nm and a surface area of 90 m^2/g (data from manufacturer Kerr-McGee Pigments). It is expected that it is a loose powder and that all aggregates in this powder are soft aggregates that break up easily.

The gas flow was varied from 0 to 2 l/min (velocities of 0-63 mm/s), and several vibration frequencies were used, ranging from 0-47 Hz. Higher gas velocities were not used because the particles started to be elutriated from the column. Pressure fluctuations were measured at a frequency of 400 Hz using piezo-electric pressure transducers, Kistler type 7261, at two heights in the column: 50 mm and 125 mm above the gas distributor. For the titania particles the data from 125 mm are given in this paper because of a blockage of the lower measuring point after some time, for the cathode particles the height of 50 mm was used due to the lower bed height. For the titania particles, the data from the higher and lower measuring point were comparable. The fluidisation experiments were done at room temperature and atmospheric pressure.

RESULTS AND DISCUSSION

Figure 4 shows the relative bed expansion during the experiments. To calculate this, the minimum bed height that was measured during all experiments was taken as the initial bed height H_0. This minimum was found when the bed was compacted at the highest vibration frequency. The measured values were 65 mm for cathode particles and 99 mm for titania. For these experiments, the vibration frequency was set to a fixed value, and the gas velocity adjusted. We started with the lowest frequency. However, the experiments were also carried out with particles with a history of vibration, also at high frequencies; these experiments are marked with a * in the figures. The graphs confirm that the initial bed height depends on the vibration frequency, at higher frequencies the particles are packed closer. Visual observations of the fluidisation behaviour of the cathode particles suggest that at low gas velocities, there is some channelling. At higher velocities, the eruptions at the bed surface are more violent and appear to originate from (small) bubbles, although these are hard to distinguish since the powder is black. The vibrations have some influence: at high frequencies bubbles start to appear at lower gas velocities. The effect was not quantified due to aforementioned visibility problems. For the (white)

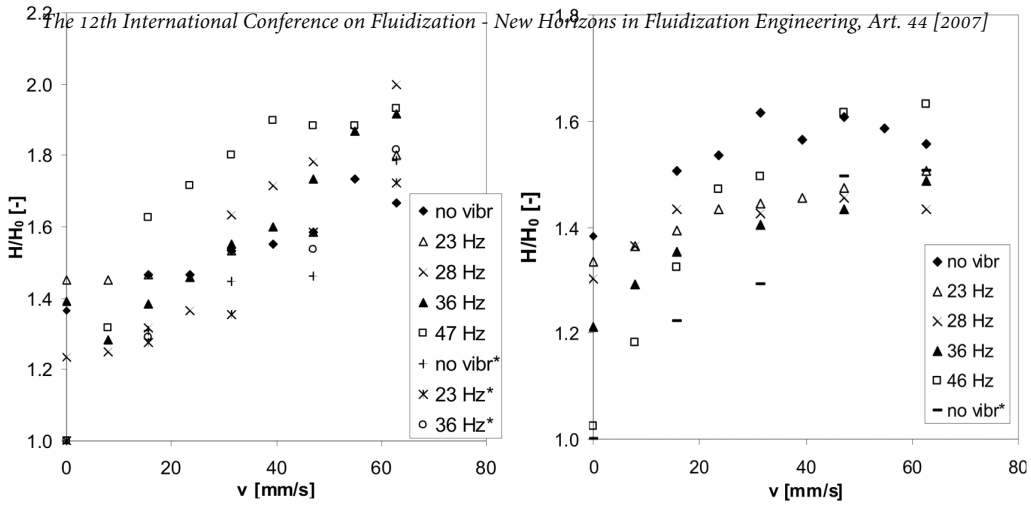

Figure 4: Relative bed heights during fluidisation at various gas velocities and vibration frequencies. Left: $LiMg_{0.05}Ni_{0.45}Mn_{1.5}O_4$; right: TiO_2-particles. Data sets labeled with a * are from particles with a vibration history.

titania powder it is easier to distinguish channels and bubbles. For each velocity and frequency, there is a certain part in the bottom of the bed that is not moving. Some large aggregates can be distinguished here and channelling occurs in between these aggregates. The height of this part decreases with gas velocity and vibration frequency. Above this bottom zone, the bed fluidises with small bubbles. A memory effect could be noticed for both particle types, although it was stronger and lasted longer for the titania. The non-moving bottom zone was much smaller for particles with a history of vibration than for 'fresh' particles. An explanation could be that part of the aggregates was broken up by the high frequencies, and only the very large (hard) aggregates remained. The bed expansion factor H/H_0 reached a maximum value of 2.0 for the cathode particles and 1.63 for the titania particles, which agrees well with literature data (11-13). It was also found that when the vibration and gas flow are stopped, the bed does not return to its initial height, and even after several days it may still be expanded (H/H_0~1.4), showing that the aggregates are very loosely packed. This effect was observed in literature as well (11). The measured porosities for the cathode particles were in the range of 0.66-0.83, and for the titania it was 0.87-0.92.

Figure 5 shows the standard deviation of the pressure signal during the experiments, which could provide information on the regime in which the fluidised bed is operating (17). The pressure fluctuations in the experiments with a high vibration frequency are determined mainly by the vibrations, the influence of the gas flow was minor. This was confirmed by the power spectrum, where high peaks occurred at the vibration frequency. When there is no vibration or vibration at a low frequency, there is a noticeable influence of the gas flow on the pressure fluctuations, as is observed in a regular gas-fluidised bed as well (17). For the cathode particles, the sudden rise followed by a decrease in the fluctuations at high frequencies could indicate a transition from bubbling to turbulent regime. However, more data are necessary to confirm this and explain the mechanism. For the TiO_2 this transition was not observed for the studied range of gas velocities. The data series from particles with a vibration history show that this history and the change in fluidisation behaviour it causes do not have a large influence the pressure fluctuations.

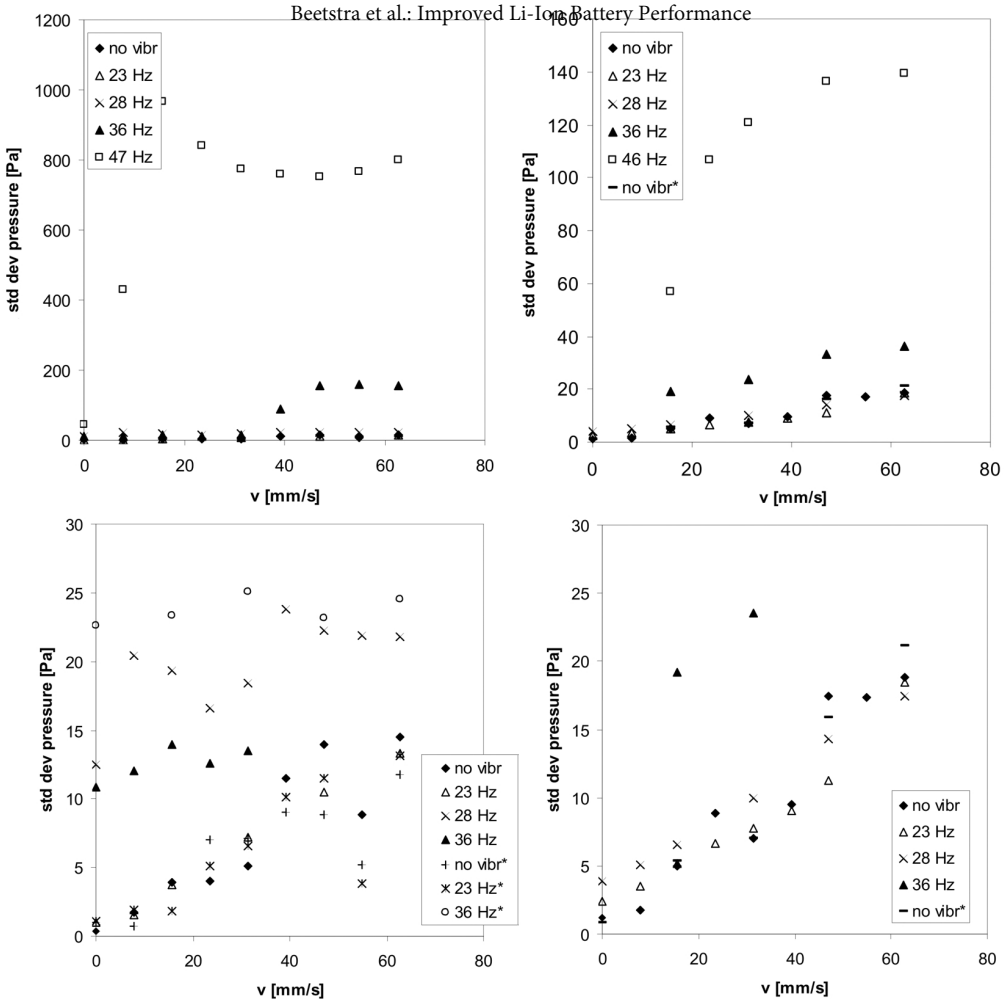

Figure 5: Standard deviation in pressure signal as a function of gas velocity. Left: $LiMg_{0.05}Ni_{0.45}Mn_{1.5}O_4$; right: TiO_2-particles. The lower pictures zoom in on the low fluctuations range. Data sets labeled with a * are from particles with a vibration

CONCLUSIONS

This paper shows the first fluidisation results of nanocrystallyne, yet aggregated, $LiMg_{0.05}Ni_{0.45}Mn_{1.5}O_4$, to be used as a cathode material in Li-ion batteries. The data are compared to commercial TiO_2-nanoparticles. The fluidisation behaviour of both particle types depends on gas velocity and vibration frequency, where a higher frequency results in a larger bed expansion (23-47 Hz). The bed expansion agrees with literature data. The cathode particles seem to be more easily fluidised as less very large agglomerates are present, although visibility for this type of particles was poor. Both materials show a history effect in their fluidisation behaviour: particles that had been vibrated at high frequencies showed a larger bed expansion and a bubbling bed was formed at lower vibration frequencies and gas velocities. This history effect did not influence the measured pressure fluctuations strongly. In the future the cathode particles will be coated with an inert layer by ALD, after which they will be tested in batteries.

The 12th International Conference on Fluidization - New Horizons in Fluidization Engineering, Art. 44 [2007]

ACKNOWLEDGEMENT

SenterNovem is acknowledged for funding this project.

REFERENCES

1. L.J. Fu, H. Liu, C. Li, Y.P. Wu, E. Rahm, R. Holze and H.Q. Wu, *Surface modifications of electrode materials for lithium ion batteries*, Solid State Sci. 8 (2006), 113-128
2. F.G.B. Ooms, E.M. Kelder, J. Schoonman, M. Wagemaker and F.M. Mulder, *High-voltage $LiMg_{\delta}Ni_{0.5-\delta}Mn_{1.5}O_4$ spinels for Li-ion batteries*, Solid Sttate Ionics 152-153 (2002), pp 143-153
3. U. Lafont, C. Locati, E.M. Kelder, *Nanopowders of spinel type electrode materials for Li-ion batteries*, EMRS 2006 Symposium Proceedings
4. T.-T. Myung, S. Komaba, N. Kumagai, H. Yashiro, H.-T. Chung and T.-H. Cho, *Nano-crystallyne $LiNi_{0.5}Mn_{1.5}O_4$ synthesized by emulsion drying method*, Electrochimica Acta 47 (2002), pp 2543-2549
5. A.M. Kannan and A. Manthiram, *Surface/Chemically Modified $LiMn_2O_4$ Cathodes for Lithium-Ion Batteries*, Electrochem Solid-State Lett. 5 (2002), pp A167-A169
6. J.R. Wank, S.M. George, A.W. Weimer, *Nanocoating individual cohesive boron nitride particles in a fluidized bed by ALD*, Powder Techn. 142 (2004), pp 59-69
7. J.R. Wank, S.M. George, A.W. Weimer, *Coating fine nickel particles with Al_2O_3 utilizing an atomic layer deposition – fluidized bed reactor (ALD-FBR)*, J. Am. Ceram. Soc. 87 (4) (2004), pp 762-765
8. T. Suntola, *Atomic Layer Epitaxy*, Materials Science Reports 4 (1989), pp 261-312
9. J.D. Ferguson, A.W. Weimer, and S.M. George, *Atomic Layer Deposition of Ultrathin and Comformal Al2O3 Films on BN Particles*, Thin Solid Films, 371 (2000), pp 95-104
10. D. Geldart, *Types of gas fluidization*, Powder Techn. 7 (1973), pp 285-292
11. C.H. Nam, R. Pfeffer, R.N. Dave and S. Sundaresan, *Aerated vibrofluidization of silica nanoparticles*, AIChE Journal 50 (no 8) (2004), 1776-1785
12. C. Zhu, G. Liu, Q. Yu, R. Pfeffer, R.N. Dave and C.H. Nam, *Sound assisted fluidization of nanoparticle agglomerates*, Powder Techn. 141 (2004), pp 119-123
13. L.F. Hakim, J.L. Portman, M.D. Casper and A.W. Weimer, *Aggregation behavior of nanoparticles in fluidized beds*, Powder Techn. 160 (2005), 149-160
14. S.M. George, J.D. Ferguson, A.W. Weimer, *Atomic layer controlled deposition on particle surfaces*, US patent 6613383 (2003)
15. S.M. George, J.D. Ferguson, A.W. Weimer, J.R. Wank, *Insulating and functionalizing fine metal-containing particles with conformal ultra-thin films*, US patent 6713177 (2004)
16. S.M. George, J.D. Ferguson, A.W. Weimer, J.R. Wank, *Nanocoated primary particles and method for their manufacture*, US patent 6913827 (2005)
17. H.T. Bi, N. Ellis, I.A. Abba and J.R. Grace, *A state-of-the-art review of gas-solid turbulent fluidization*, Chem. Eng. Sci. 55 (2000), pp 4789-4825